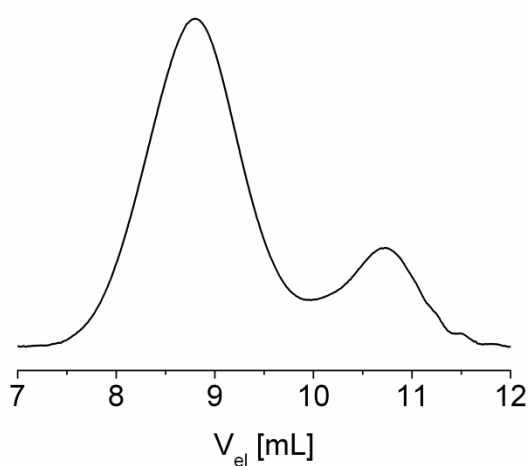


# Unexpected radical polymerization behavior of oligo(2-ethyl-2-oxazoline) macromonomers

Christine Weber, Krzysztof Babiuch, Sarah Rogers, Igor Y. Perevyazko, Richard Hoogenboom\*,  
Ulrich S. Schubert\*

## Supporting information



**Figure SI-1:** SEC trace (CHCl<sub>3</sub>, RI detection) from the reaction solution of the FRP of OEtOxA.  $M_n = 6,080 \text{ g mol}^{-1}$ ; PDI = 1.18, conv. = 81%,  $M/AIBN = 240$  (similar to  $M/CTA = 60$  from RAFT),  $[M] = 0.5 \text{ M}$  in EtOH,  $T = 70 \text{ }^\circ\text{C}$ ,  $t = 17.5 \text{ h}$ .

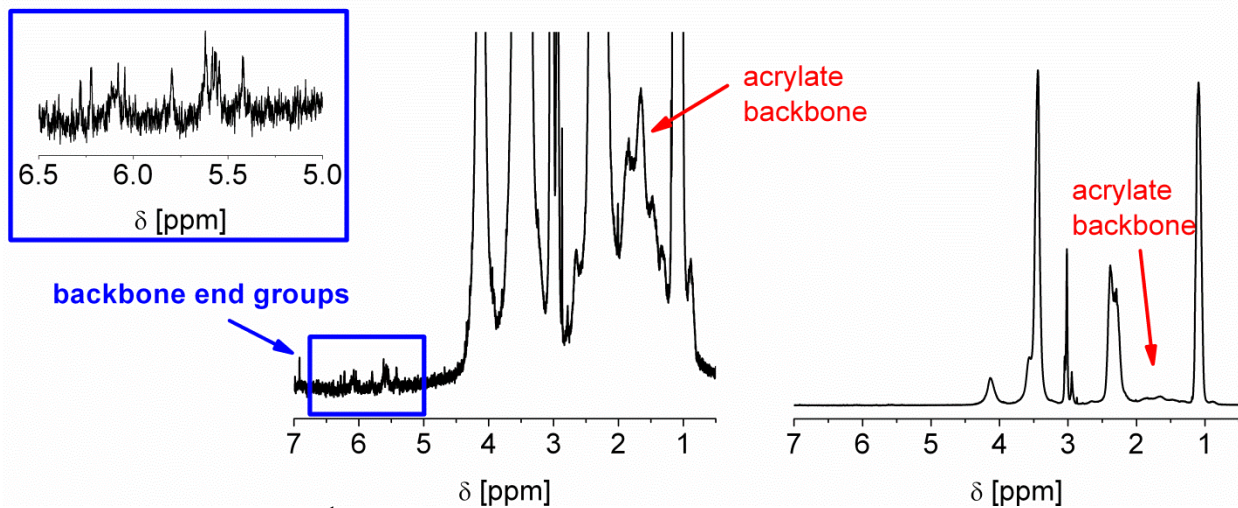


**Figure SI-2:** zoom into the  $^1\text{H}$  NMR spectrum ( $\text{CDCl}_3$ , 300 MHz) of **P3** indicating the presence of vinylic backbone end-groups.

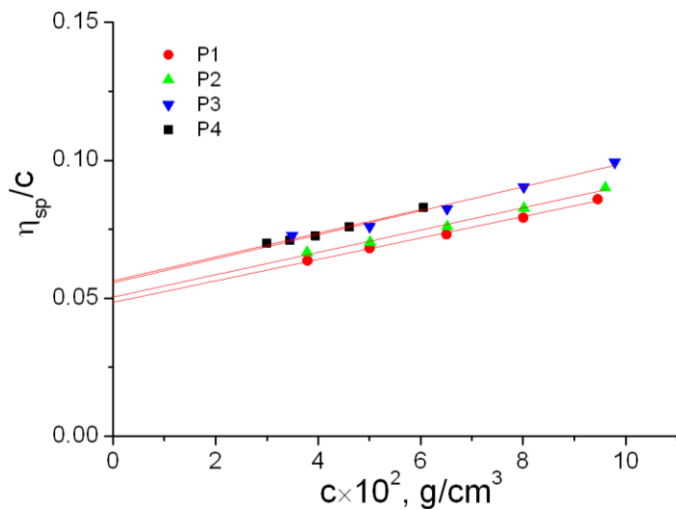


**Figure SI-3.** Dependence of  $\eta_{sp}/c$  on the solute concentration for the determination of the intrinsic viscosity.

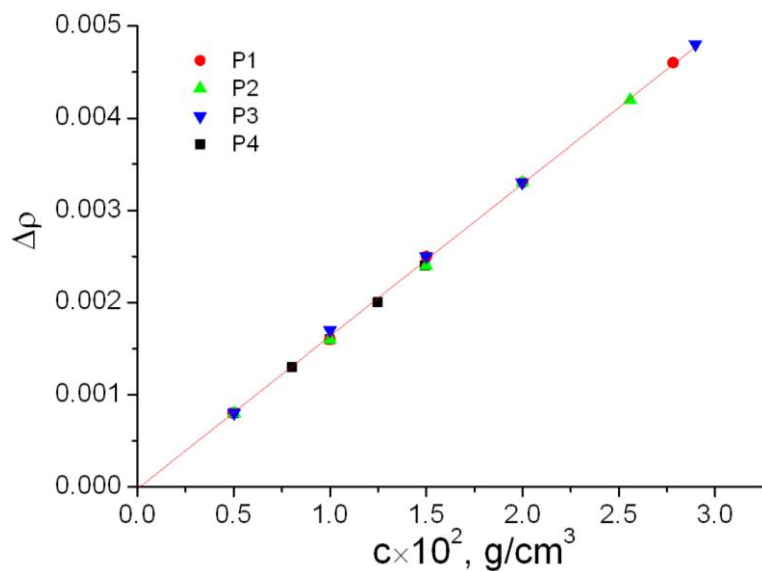


**Figure SI-4.** Dependence of  $\Delta\rho = (\rho - \rho_0)$  on the solute concentration, where  $\rho$  and  $\rho_0$  are the density of the solution and solvent respectively. The slope  $\Delta\rho/\Delta c$  corresponds to the buoyancy factor  $(1 - \nu\rho_0) = 0.166 \pm 0.01$ , which yields  $\nu = 0.835 \pm 0.004 \text{ cm}^3 \cdot \text{g}^{-1}$  for the partial specific volume.

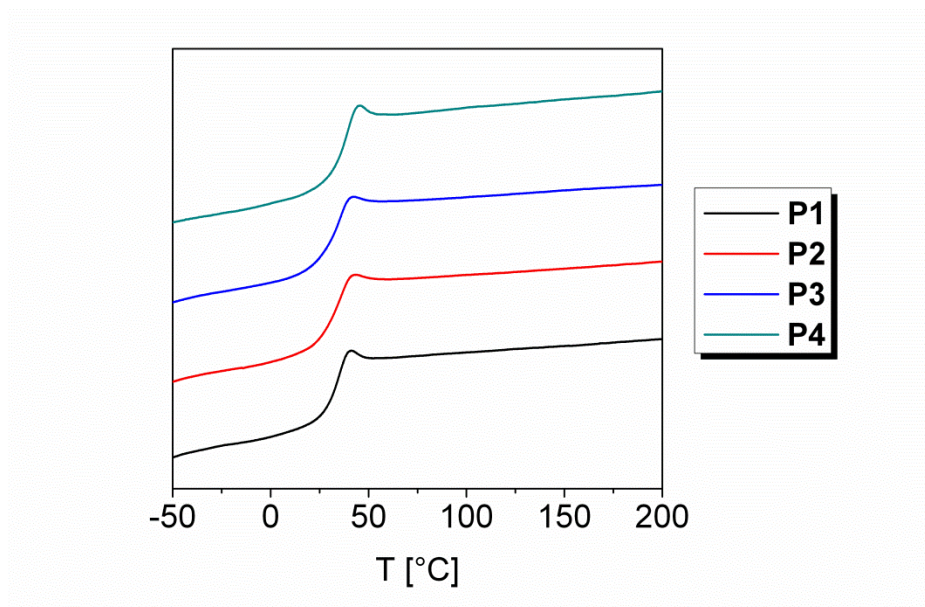


**Figure SI-5:** DSC thermograms of **P1-P4** (second heating run, heating rate  $20 \text{ K min}^{-1}$ ).

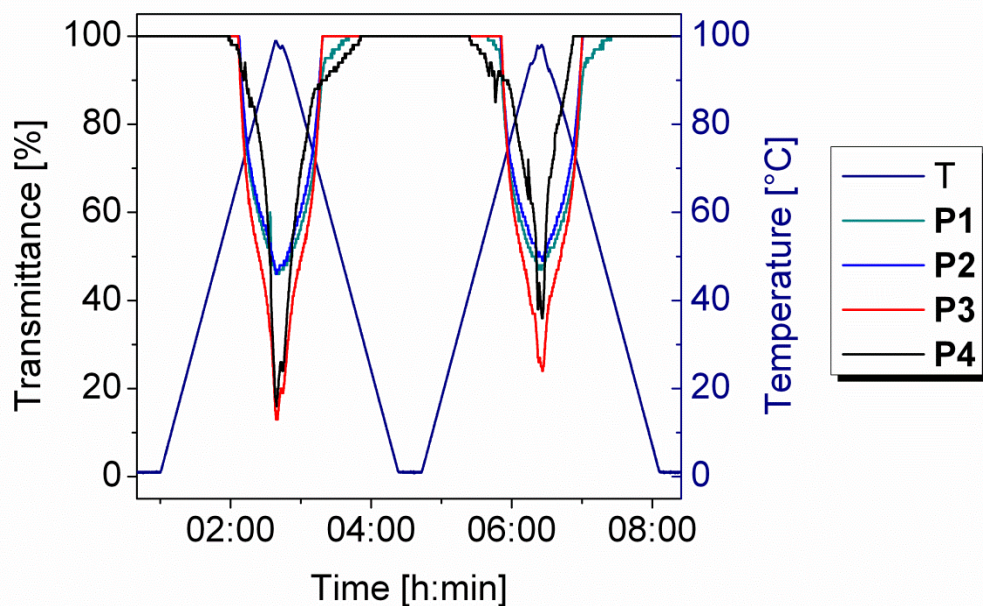


**Figure SI-6:** Turbidity curves of aqueous solutions of POEtOxA **P1-P4** ( $c = 5 \text{ mg mL}^{-1}$ , heating rate  $1 \text{ K min}^{-1}$ ).

**Table SI-1:** Parameters obtained by FISH model fitting of the SANS data for **P1-P4** in  $\text{D}_2\text{O}$ .

	Ellipsoid <sup>a</sup>			Rod <sup>b</sup>		Rod Theo.		Ellipse or Rod?
	$R_1 / \text{Å}$	X	$R_2 / \text{Å}$	$R / \text{Å}$	$L / \text{Å}$	$R / \text{Å}$	$L / \text{Å}$	
<b>P1</b>	7.9	3.9	30.8	10.2	44.5	22	20	Rod
<b>P2</b>	8.6	4.0	34.4	13.0	47.6	22	37	Rod
<b>P3</b>	12.8	3.2	41.0	12.2	60.8	22	110	Rod
<b>P4</b>	15.7	2.6	40.8	14.2	62.1	22	276	Rod

<sup>a</sup>  $R_1$  and  $R_2$  are the radii of the ellipse, and  $X = R_2/R_1$ .

<sup>b</sup> R corresponds to the radius and L to the length of the rod.

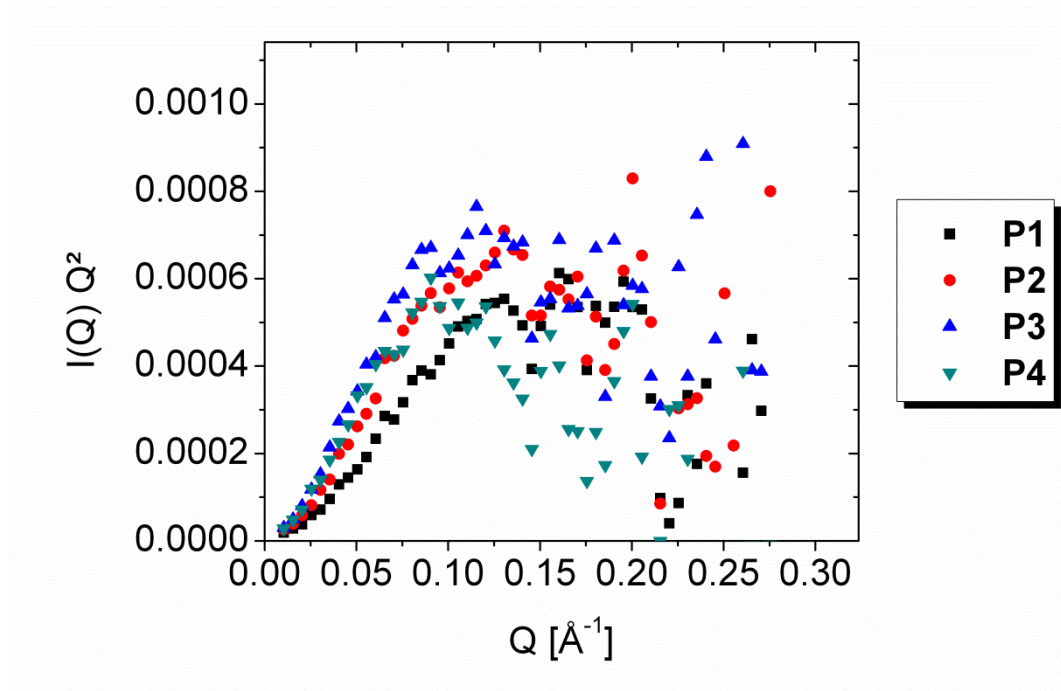


**Figure SI-7:** Kratky plots for SANS data of solutions of **P1-P4** in  $\text{D}_2\text{O}$  ( $c = 5 \text{ mg mL}^{-1}$ ).

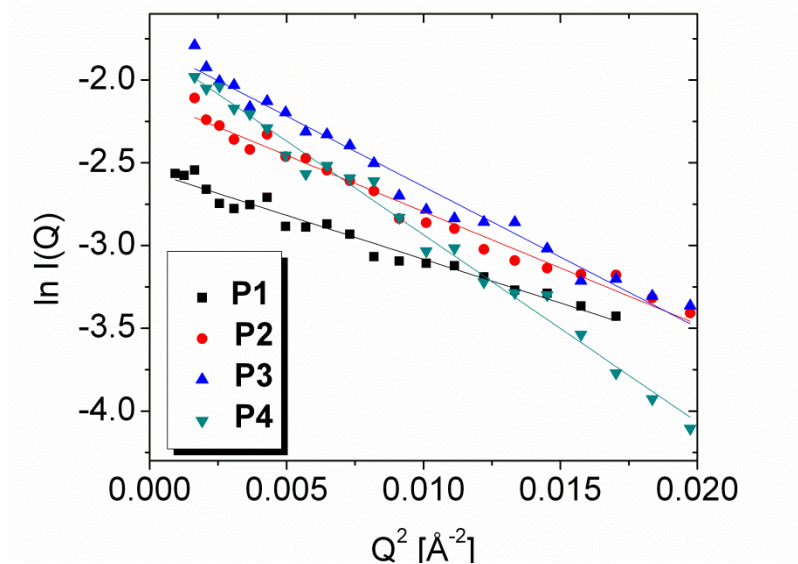


**Figure SI-8:** Guinier plot for SANS data of **P6** in  $\text{D}_2\text{O}$  ( $c = 5 \text{ mg mL}^{-1}$ ). The radius of gyration  $R_g$  is calculated from the slope of the linear fit according to  $R_g = \sqrt{-3 \cdot \text{slope}}$  in the low  $Q$  range.

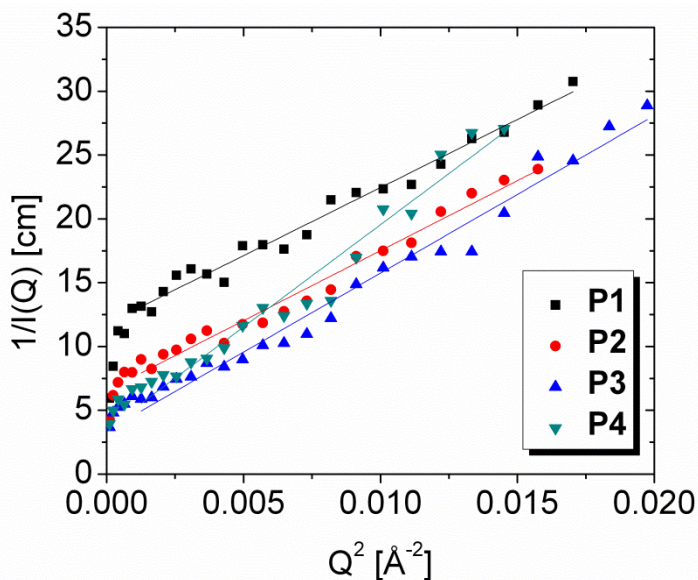


**Figure SI-9:** Zimm plots for SANS data of **P1-P4** in D<sub>2</sub>O ( $c = 5 \text{ mg mL}^{-1}$ ). The correlation length  $\xi$  is obtained from linear fitting according to  $\xi = \sqrt{\text{slope}/\text{intercept}}$  and was used to calculate  $R_g$ .

**Table SI-2.** Radii of gyration ( $R_g$ ) calculated from linear fitting of the Zimm and Guinier plots of the SANS data of **P1-4** in D<sub>2</sub>O.

	$I_0 [\text{cm}^{-1}]$	$\xi [\text{Å}]^a$	$R_g [\text{Å}]$ Zimm (low Q) <sup>b</sup>	$R_g [\text{Å}]$ Zimm (high Q) <sup>c</sup>	$R_g [\text{Å}]$ Guinier	$R_g [\text{Å}]$ cyl. fit <sup>d</sup>	$R_g [\text{Å}]$ ell. fit <sup>e</sup>
<b>P1</b>	0.085	9.5	16	13	13	14	15
<b>P2</b>	0.15	13	22	18	15	15	17
<b>P3</b>	0.29	19	33	27	17	18	20
<b>P4</b>	0.28	21	37	30	19	18	21

<sup>a</sup> correlation length obtained from Zimm analysis.

<sup>b</sup> calculated according to  $R_g = \xi\sqrt{3}$ .

<sup>c</sup> calculated according to  $R_g = \xi\sqrt{2}$ .

<sup>d</sup> calculated according to  $R_g = \sqrt{\frac{L^2}{12} + \frac{R^2}{2}}$  from the cylindrical fit.

<sup>e</sup> calculated according to  $R_g = \sqrt{\frac{2R_1^2 + 2R_2^2}{5}}$  from the ellipsoid fit.